



Inhibitory effect of different product analogues on β -alanine synthase: A thermodynamic and fluorescence analysis

Montserrat Andújar-Sánchez, Ana Isabel Martínez-Gómez, Sergio Martínez-Rodríguez, Josefa María Clemente-Jiménez, Francisco Javier Las Heras-Vázquez, Felipe Rodríguez-Vico, Vicente Jara-Pérez*

Departamento de Química Física, Bioquímica y Química Inorgánica, Facultad de Ciencias Experimentales, Universidad de Almería, Carretera de Sacramento s/n, La Cañada de San Urbano, Almería 04120, Spain

ARTICLE INFO

Article history:

Received 9 July 2008

Received in revised form 16 September 2008

Accepted 19 September 2008

Available online 4 October 2008

Keywords:

Isothermal titration calorimetry
N-Carbamoyl- β -alanine amidohydrolase
 β -Ureidopropionase
 Fluorescence
 Inhibition

ABSTRACT

The enzyme *N*-carbamoyl- β -alanine amidohydrolase catalyse the hydrolysis of *N*-carbamoyl- β -alanine or *N*-carbamoyl- β -aminoisobutyric acid to β -alanine or 3-aminoisobutyric acid, under the release of carbon-dioxide and ammonia. This work studies the inhibition of *N*-carbamoyl- β -alanine amidohydrolase from *Agrobacterium tumefaciens* C58 (At β car) by different carboxylic acid compounds that differ in number of carbons, and position and size of ramification, while the binding thermodynamics of the inhibitors are studied by isothermal titration calorimetry (ITC) and fluorescence. From the binding constants and inhibition studies, we conclude that propionate is the most efficient inhibitor among those tested. Substitution of the linear alkyl acids in positions 2 and 3 resulted in a drastic decrease of the affinity. The thermodynamic parameters show that a conformational change is triggered upon ligand binding. Binding enthalpy ΔH_b is negative in all cases for all ligands, and thus, Van der Waals interactions and hydrogen bonding are most probably the major sources for this term. The process is entropically favoured at all temperatures and pH studied, most probably due to the liberation of water molecules accompanying the conformational change of the enzyme.

© 2008 Elsevier Ltd. All rights reserved.

1. Introduction

The enzyme *N*-carbamoyl- β -alanine amidohydrolase (Nc β aa, E.C. 3.5.1.6), also known as β -alanine synthase and β -ureidopropionase, acts as the last enzyme in the reductive pyrimidine-degradation pathway, where uracil and thymine are degraded to the corresponding β -amino acids, β -alanine, and 3-aminoisobutyric acid. This pathway has been commonly generalized as catabolic, although it can also function as a significant biosynthetic route for β -alanine production. The latter is a precursor of coenzyme A (CoA) and pantothenic acid in bacteria and fungi (vitamin B5) [1] and is widely distributed in the central nervous system of vertebrates; as a structural analogue of γ -amino-*n*-butyric acid and glycine, major inhibitory neurotransmitters, it has been suggested that it may be involved in synaptic transmissions [2].

The Nc β aa from different sources has been reported to be inhibited by product analogues [3–5]. Furthermore, *in vivo* experiments have shown that inhibition of the human enzyme by propionic acid (which can be accumulated due to propionic academia) could be related to neurological complications due to decreased β -alanine

production [5]. As far as we know, despite the biological relevance that this enzyme might have, no thermodynamic or detailed inhibition studies have been carried out on the interaction of these analogues for any Nc β aa. Recently, we have characterised the Nc β aa from *Agrobacterium tumefaciens* C58 (At β car) showing activity towards different substituted and non-substituted *N*-carbamoyl- α , β , γ , and δ -amino acids (Martínez-Gómez *et al.*, work in preparation). Due to its broad substrate-spectrum, we decided to use this enzyme to carry out inhibition studies with different product analogues. Several compounds different from propionate in number of carbons and kind of ramification were selected to study their inhibitory effect and the influence of these changes on affinity. ITC and fluorescence were used to obtain thermodynamic information related to the binding process, and modelling studies were carried out in conjunction to try to explain the thermodynamic and inhibitory behaviour.

2. Materials and methods

2.1. Materials

All chemicals were of analytical grade, and were used without further purification. TALON™ metal affinity resin was purchased

* Corresponding author. Tel.: +34 950 015316; fax: +34 950 015008.
 E-mail address: vjara@ual.es (V. Jara-Pérez).

from Clontech Laboratories, Inc. Buffer reagent sodium phosphate and carboxylic acids were purchased from Sigma Aldrich Quimica (Madrid, Spain).

2.2. Apoenzyme and holoenzyme preparation

The At β car was purified by cobalt affinity as previously reported (Martinez-Gomez *et al.*, work in preparation). Briefly, the recombinant enzyme was overproduced in *Escherichia coli*, including a His6-tag and purified using TALON™ metal affinity resin (CLONTECH Laboratories, Inc.). The purified enzyme was dialysed against 0.1 M sodium phosphate pH 8.0 and stored at $T = 277$ K, until use.

The apoenzyme was prepared by incubating (45 to 50) μ M of purified At β car with 10 mM of 8-hydroxyquinoline-5-sulphonic acid (HQSA) at $T = 277$ K overnight. The HQSA was removed by dialysis in four stages at 12-h intervals, all at $T = 277$ K and using the corresponding buffers for ITC or fluorescence experiments (described below).

Activity of At β car required the presence of divalent metal ions such as Ni^{2+} (Martinez-Gomez *et al.*, work in preparation). To obtain the holoenzyme, (20 to 50) μ M apoenzyme were dialyzed with the buffer to be used for the corresponding experiment, adding 0.5 mM NiCl_2 in the last dialysis step, from a 100 mM stock solution.

2.3. Primary sequence analysis and modelling studies

The multiple amino acid sequence alignment was performed with ClustalW [6], using the sequences of At β car, β -alanine synthase from *Saccharomyces Kluyveri* (Sk β as), and ι -carbamoylase from *Sinorizobium meliloti* (SmeLcar). The alignment was used as an input for ESPrit utility [7], together with the structure of β -alanine synthase from *Saccharomyces Kluyveri* (Sk β as, PDB 1R3N). The At β car open model was obtained by Swiss-model server [8], using the structure of Sk β as (PDB 1R3N) as the template [2]. The model of the closed conformation was obtained previously (Martinez-Gomez *et al.*, work in preparation) with the Swiss-model server along to the substrate-bound structure of Sk β as (PDB 2V8H) as template, which has been solved at $2.0 \cdot 10^{-10}$ m [9].

The stereochemical geometry of the final model was validated by PROCHECK [10] and WHATCHECK [11]. Manual model building of the structures was performed with Swiss PDB viewer [12] and pymol [13].

2.4. Inhibition studies

Inhibition studies were carried out incubating the holoenzyme (5 μ M) at At β car 277 K for 60 min with and without the different carboxylic acids (final concentration 10 mM), in 100 mM phosphate buffer pH 8.0 (final volume 0.400 cm^3). This solution was afterwards preincubated for 1 min at $T = 303$ K and 0.100 cm^3 of 100 mM ι -N-carbamoyl- α -tryptophan (at the same temperature, prepared in 100 mM phosphate buffer pH 8.0) were added to measure enzymatic activity. Aliquots (0.050 cm^3) were retrieved after (5, 10, 20, and 30) min, and reaction was stopped by adding 0.450 cm^3 of 1% H_3PO_4 . After centrifuging, the resulting supernatants were analysed by high performance liquid chromatography (HPLC). The HPLC system (Finnigan SpectraSYSTEM HPLC System, Thermo, Madrid, Spain) equipped with a LUNA 5 μ m C18(2) column (4.6 mm \times 250 mm, Phenomenex) was used to detect ι -tryptophan. The mobile phase was 20 mM H_3PO_4 pH 3.2:methanol (80:20 v/v), pumped at a flow rate of 0.75 $\text{cm}^3 \cdot \text{min}^{-1}$ and measured at 273 nm.

2.5. Isothermal titration calorimetry

Titration were performed using the MCS high-sensitive microcalorimeter manufactured by Microcal Inc. (Microcal, Northampton,

MA, USA), which has been described elsewhere [14,15]. A circulating water bath (Neslab RTE-111) was used to stabilise the temperature. The instrument was allowed to equilibrate overnight. The enzyme was dialyzed extensively against 100 mM sodium phosphate, 0.5 mM NiCl_2 (or without NiCl_2 for experiments with apoenzyme) at pH 6 and 7 (and pH 8 for propionate) prior to all titrations. The ligands were prepared in the final dialysis buffer. The enzyme was loaded into the sample cell of the calorimeter ($V = 1.38 \text{ cm}^3$) using enzyme concentrations from (17.96 to 32.73) μ M, while concentrations of inhibitors ranged from (66.17 to 77.44) mM for formate, from (20.85 to 53.4) mM for acetate, from (19.6 to 42.3) mM for propionate, and from (74.8 to 81.5) mM for butyrate.

The system was allowed to equilibrate and a stable baseline was recorded before initiating an automated titration. The titration experiment consisted of 25 injections of 10 cm^3 each into the sample cell, carried out at 4-min intervals at different temperatures. The sample cell was stirred at 400 rpm. Dilution experiments were performed by identical injections of different carboxylic acids into the cell containing only buffer. The thermal effect of protein dilution was negligible in all cases. The peaks of the thermograms obtained were integrated using the ORIGIN software (Microcal, Inc.) supplied with the instrument.

2.6. Fluorescence studies

2.6.1. Determination of binding constants

Fluorescence emission spectra were measured at $T = 298.15$ K in a Perkin Elmer LS55 spectrofluorimeter for At β car in 100 mM sodium phosphate, 0.5 mM NiCl_2 , pH 7. The temperature of the cell holder was controlled with a circulating water bath. Protein samples (0.3 μ M) were excited at (280 and 295) nm to characterize a different behaviour of tryptophan and tyrosine residues. The binding of different substrates to the enzyme was monitored by using the decrease in fluorescence emission at 350 nm. Excitation and emission bandwidths were 4 nm. Fluorescence measurements were corrected for dilution. The saturation fraction, Y , can be expressed as

$$Y = (K \cdot [\text{Ligand}]) / (1 + K \cdot [\text{Ligand}]), \quad (1)$$

where K is the characteristic microscopic association constant and $[\text{Ligand}]$ the free concentration of inhibitors, which can be expressed as

$$[\text{Ligand}] = [\text{Ligand}]_T - n \cdot Y \cdot [\text{Enzyme}], \quad (2)$$

where $[\text{Ligand}]_T$ is the total concentration of inhibitor, n the number of active sites, and $[\text{Enzyme}]$ the concentration of At β car. The saturation fraction, Y , can be calculated as

$$Y = (F(\text{Ligand}) - F(0)) / (F(\infty) - F(0)), \quad (3)$$

where $F(0)$, $F(\text{Ligand})$, and $F(\infty)$ are the corrected fluorescence intensities for the protein solution without ligand, at concentrations of ligand equal to those of inhibitors, and at saturating ligand concentration, respectively.

2.6.2. Urea unfolding experiments

Unfolding studies with urea as denaturant were performed at pH (6, 7, and 8) (in 100 mM sodium phosphate, 0.5 mM NiCl_2). Protein concentration was (0.2 to 0.3) μ M and the concentration range of denaturant used was (0 to 6) M. Denaturant concentrations were determined by measuring the index of refraction with a refractometer (Refracto 30GS, Mettler Toledo, Germany) and applying the following equation:

$$[\text{Urea}] / M = 117.66\Delta n + 29.753\Delta n^2 + 185.56\Delta n^3, \quad (4)$$

where Δn is the difference between index of refraction of the buffer at a particular urea concentration and the index of refraction of the buffer in absence of urea.

Equilibrium times for the unfolding transition enzyme were determined by following changes in intrinsic fluorescence. A 24 h pre-incubation time was used prior to the fluorescence measure-

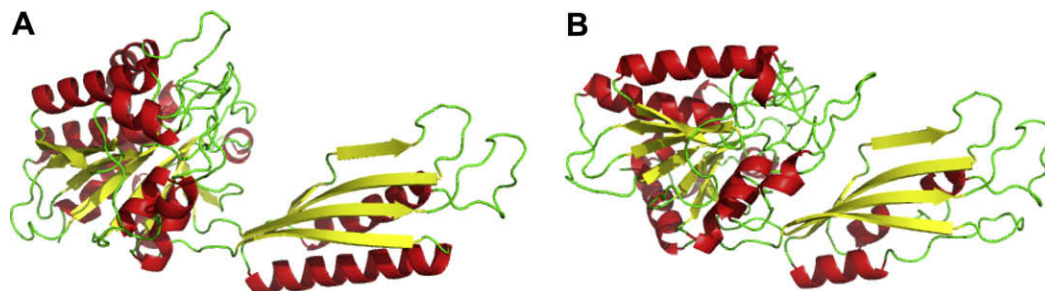


FIGURE 1. Overall topologies of (A) open and (B) closed monomer of Atβcar, showing how the catalytic domain approaches the lid domain upon substrate binding, thus generating a more hydrophobic environment which would explain the negative values of enthalpic contribution.

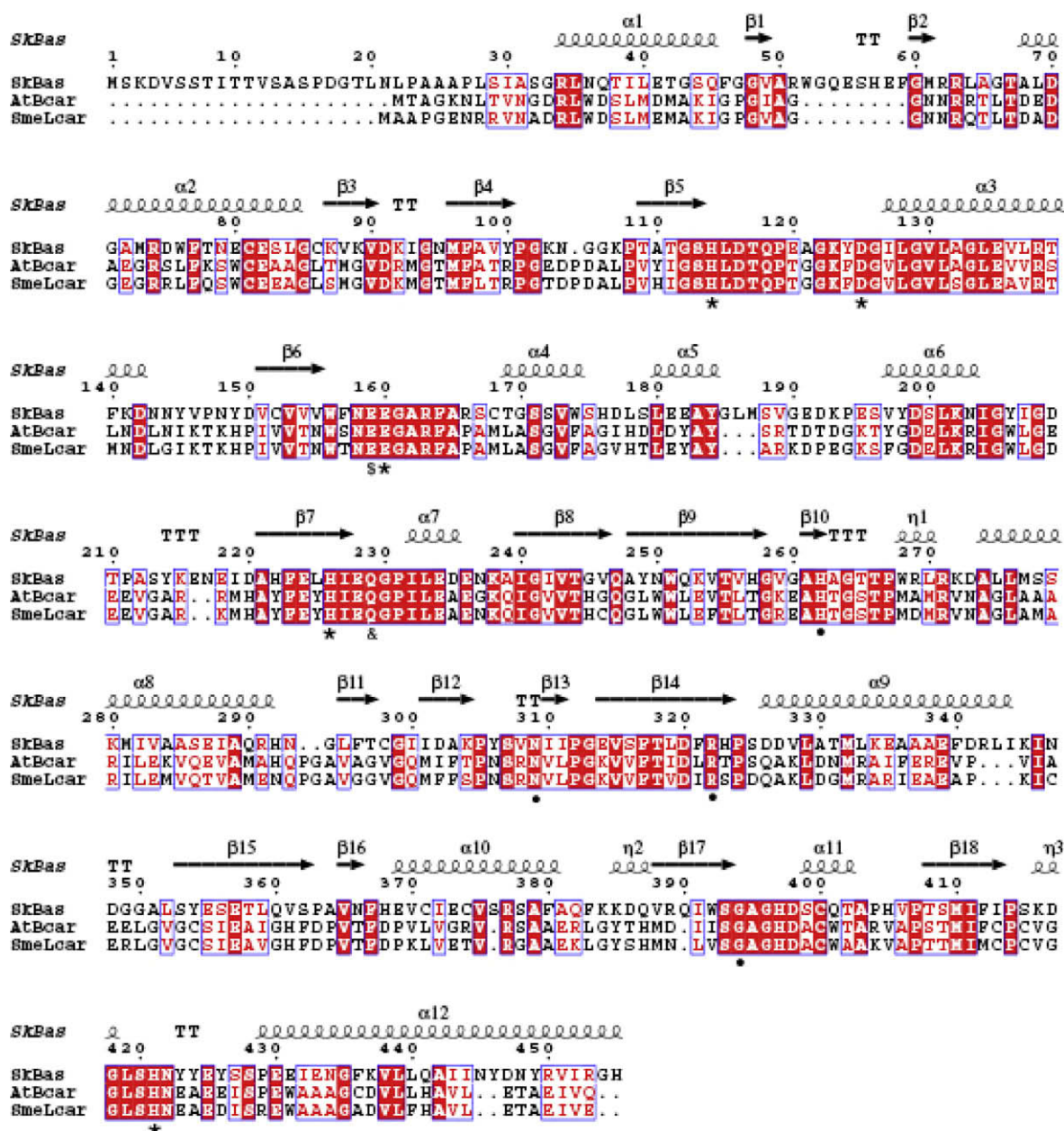


FIGURE 2. Sequence alignment showing the catalytic residues conserved between Atβcar (GenBank accession No. EF507843), Skβas (GenBank accession No. AAK60518), and SmeLcar (GenBank accession No. AAT66633). Their different roles are as follows: * metal binding; \$ substrate binding; and S hydrolyzing hydroxyl group activation.

ments to ensure that the denaturation equilibrium was reached, as observed by variations in the λ_{\max} of the spectra. Samples were then incubated at $T = 298$ K for 30 min just before measurements.

The profiles of fluorescence intensity versus denaturant concentration were analysed according to a two-state denaturation model [16], in agreement with the experimental results found by gel filtration. The free energy of denaturation of proteins in the presence of denaturant, ΔG , is linearly related to the concentration of denaturant

$$\Delta G = \Delta G_w - mC \quad (5)$$

Taking into account equilibrium between the dimer and monomer, ΔG_w can be calculated from

$$\Delta G_w = -mC_{1/2} - RT \ln[M], \quad (6)$$

where $C_{1/2}$ is the concentration of denaturant at which half of the protein is denatured, m is the slope of the transition, and $[M]$ the monomer concentration (twice the dimer concentration).

2.6.2.1. Urea unfolding followed by gel filtration chromatography. Gel filtration chromatography was performed in an AKTA BASIC FPLC system (GE-Healthcare), using a Superdex 200 HR 10/30 column (Amersham Biosciences, Barcelona, Spain) at a flow speed of $0.5 \text{ cm}^3 \cdot \text{min}^{-1}$ and monitored at 280 nm. The column was equilibrated with 100 mM sodium phosphate, 0.5 mM NiCl_2 pH 7 at different concentrations of urea (0, 2, 4, and 6) M. Samples of At β car (134 μM in protomer units) were preincubated overnight at $T = 277$ K at the same concentrations of urea used for elution.

3. Results and discussion

3.1. Sequence and structural analysis of At β car

Structural models for At β car were determined using the known free (open) and bound (closed) structures of Sk β as (1R3N and 2V8H, respectively), using Swiss-model server [8]. Similar overall topologies were obtained to those observed for the X-ray structures of Sk β as (figure 1). Out of a total of 415 residues, the final models included 409 and 378 residues for the open and closed models, respectively. The omitted residues are at the N (5 and 30 residues) and C (1 and 7 residues) termini.

By analogy with Sk β as, At β car would present two domains (figure 1); a large domain comprising residues 2–213 and 331–415, namely the “catalytic domain”, and a smaller domain formed by residues 214–330, called “lid domain”. The catalytic residues previously reported for two members of this family of enzymes (Sk β as and SmeLcar, [16,17]) are completely conserved for At β car (figure 2). In the latter, the binuclear-metal centre would be formed by His86, Asp97, Glu132, His193, and His385. Residues Arg291, His229, and Asn278 would be responsible for the recognition of the carboxyl moiety of the substrate/inhibitor, while Gly360 and Gln196 would allocate the ureido group inside the catalytic centre in the correct position for its hydrolysis. The Glu131 would be the nucleophilic group responsible for proton abstraction of a water molecule bridging both metallic atoms in the catalytic centre, thus generating an “activated” hydroxyl group able to hydrolyze the carbamoyl group of the substrate.

3.2. Relative molecular mass and subunit structure

The relative molecular mass was calculated as (90 to 92) kDa at pH (6, 7, and 8) by Gel Filtration using a Superdex 200 HR 10/30 column. The relative molecular mass of the subunit was estimated to be 45 kDa by SDS/PAGE. These data suggest that the native enzyme consists of two subunits with identical molecular mass.

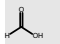
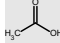
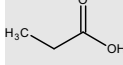
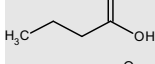
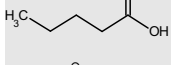
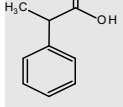
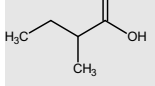
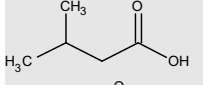
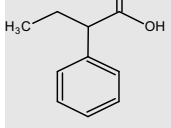
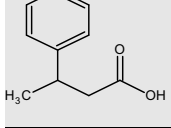
The same biological unit has been found for Sk β as [17] and *Pseudomonas putida* Nc β aa [4].

The aggregation state of the enzyme was not altered by the presence of formiate, acetate, propionate, or butyrate at saturation conditions (data not shown).

3.3. Inhibitory effect of different carboxylic acids on At β car

In order to evaluate the inhibition caused by different product analogues, inhibition studies were carried out with different carboxylic acids. All the assayed compounds decreased the activity of the enzyme (table 1). The inhibitory effect depended on: (1) the length of the linear alkyl-chain, and (2) the size and position of the ramification. Among the linear alkyl acids, propionate was found to be the best inhibitor. In Sk β as, a conformational change in the catalytic domain is triggered upon substrate binding, approaching it to the lid domain of the counterpart monomer, inserting the ureido-moiety of the substrate into the binuclear-metal centre of the enzyme, where the hydrolysis takes place [9]. A single arginine residue belonging to the lid domain (Arg291 in At β car) has been proven as the key residue responsible for sub-

TABLE 1
Relative activity (%) of At β car in the presence and absence of the different inhibitors

Inhibitor structure/name	Relative activity/%
Without (control)	100.00 \pm 0.00
 Formiate	97.45 \pm 1.45
 Acetate	69.92 \pm 1.76
 Propionic acid	50.80 \pm 0.59
 Butyric acid	71.71 \pm 2.93
 Valeric acid	75.40 \pm 1.72
 2-Phenylpropionic acid	70.33 \pm 3.01
 2-Methylbutyric acid	55.16 \pm 2.09
 Isovaleric acid	78.83 \pm 2.00
 2-Phenylbutyric acid	79.89 \pm 3.10
 3-Phenylbutyric acid	78.02 \pm 0.78

Measurements were carried out in triplicate with different batches of the enzyme.

strate binding in at least two members of the peptidase family [9,17], although other non-indispensable binding residues appearing in the counterpart monomer are involved in this task (His229, Asn278 for Atβcar). By analogy with the other members, it can be inferred that these residues are responsible for inhibitor binding: the carboxyl group of the acids used would bind those residues blocking the binding of the *N*-carbamoyl-β-amino acid, and thus the enzymatic activity.

3.4. Binding of linear alkyl acids

In order to study the influence of inhibitor chain length in the binding process, we tested different product analogues differing in one methylene group each. The ITC experiments were conducted at two different pHs (6 and 7) (and pH 8 for propionate) and different temperatures to determine the thermodynamic parameters of the binding of these compounds to Atβcar (table 2). No large differences were revealed between thermodynamic parameters at pHs 6 and 7. The affinity constants follow the same trend found in the inhibition studies. Binding could be detected up to four-member ligands, but not with longer chain compounds, (valeric acid caused around 25% of inhibition, although affinity constant was too small to analyze the data). A typical profile of the binding of propionate to the enzyme is shown in figure 3A. figure 3B includes a plot of the total heat evolved per mole of the ligand versus the ratio inhibitor concentration over enzyme concentration. The smooth solid line represents the best fit of the experimental data to a model of two equal and independent sites (one per monomer) in agreement with Atβcar biological unit, showing one catalytic cleft per mono-

mer. In this model total heat evolved in the titration after *i* titrations, $Q(i)$, is given by

$$Q = \frac{nM_t \Delta H V_0}{2} \left[1 + \frac{X_t}{nM_t} + \frac{1}{nKM_t} - \sqrt{\left(1 + \frac{X_t}{nM_t} + \frac{1}{nKM_t} \right)^2 - \frac{4X_t}{nM_t}} \right], \quad (7)$$

where K is the binding constant, n the number of sites, V_0 the active cell volume, M_t the bulk concentration of macromolecule in V_0 , and X_t the bulk concentration of ligand.

The parameter of greatest interest for comparison with the experiment, however, is the change in heat from the completion of injection $i - 1$ to the completion of injection i . The correct expression then for heat released, $\Delta Q(i)$, from the *i*th injection is

$$\Delta Q(i) = Q(i) + \frac{dV_i}{V_0} \left[\frac{Q(i) - Q(i-1)}{2} \right] - Q(i-1). \quad (8)$$

Since ΔH_b is negative in all cases for all ligands, binding of Atβcar to formate, acetate, propionate, and butyrate at these two pHs is exothermic. Van der Waals interactions and hydrogen bonding are usually considered to be the major potential sources of negative ΔH values. Before binding, the inhibitor might be forming H bonds with the water molecules of the solvent. After binding, the inhibitor might also be forming hydrogen bonds with the groups of amino acids of the active site. Thus, the binding of carboxyl group of the ligand to residue Arg291 of the monomer forms a salt bridge, as does hydrogen bonding to residues His229 and Asn278 of the other monomer [17]. These H bonds are formed in a more apolar medium than water and may be the major contribution to the intrinsic

TABLE 2

Thermodynamic parameters and binding constants determined by ITC and fluorescence for the binding of formate, acetate, propionate, and butyrate to Atβcar at different temperatures and pH

Substrate	pH	T/K	$\Delta H/(\text{J} \cdot \text{mol}^{-1})$	$\Delta C_p/(\text{J} \cdot \text{mol}^{-1} \cdot \text{K}^{-1})$	$K/M^{-1}(\text{ITC})$	$\Delta G/(\text{kJ} \cdot \text{mol}^{-1})$	$\Delta S/(\text{J} \cdot \text{K}^{-1} \cdot \text{mol}^{-1})$	$K/M^{-1}(\text{fluorescence})$	
Formiate	6	289.5	-1337.3 ± 85.4	-154.2 ± 11.2	893.0 ± 25.6	-16.4 ± 0.1	52.0 ± 0.1	515.6 ± 52.3	
		293.1	-1834.9 ± 90.1		814.1 ± 32.6	-16.3 ± 0.1	49.4 ± 0.1		
		298.3	-2421.7 ± 32.1		793.2 ± 20.1	-16.5 ± 0.1	47.2 ± 0.2		
		303.4	-3540.1 ± 48.3		639.5 ± 14.3	-16.3 ± 0.1	42.1 ± 0.2		
	7	289.3	-946.7 ± 46.5	-207.6 ± 10.3	594.8 ± 11.3	-15.4 ± 0.1	49.9 ± 0.2	433.7 ± 48.6	
		294.0	-1805.9 ± 34.5		531.0 ± 15.2	-15.3 ± 0.1	45.9 ± 0.2		
		298.5	-2684.8 ± 29.5		571.3 ± 21.2	-15.7 ± 0.1	43.6 ± 0.2		
		303.4	-3849.1 ± 25.2		546.4 ± 18.9	-15.8 ± 0.1	39.4 ± 0.2		
	Acetate	6	288.8	-1318.2 ± 20.3	-215.3 ± 8.6	4508.0 ± 35.8	-20.2 ± 0.1	65.2 ± 0.3	3998.8 ± 69.7
			293.3	-2163.6 ± 46.6		4309.0 ± 25.6	-20.4 ± 0.1	62.2 ± 0.2	
			298.4	-3110.5 ± 34.6		4239.0 ± 21.4	-20.7 ± 0.1	59.0 ± 0.2	
			303.2	-4235.9 ± 25.8		4008.0 ± 35.2	-20.8 ± 0.1	54.6 ± 0.2	
7		289.8	-1312.2 ± 17.7	-253.2 ± 7.5	4166.0 ± 31.6	-20.1 ± 0.1	64.8 ± 0.3	3795.3 ± 70.6	
		293.4	-2582.4 ± 23.6		4006.0 ± 32.5	-20.2 ± 0.1	60.1 ± 0.3		
		298.2	-3384.9 ± 24.7		4000.0 ± 21.8	-20.5 ± 0.1	57.4 ± 0.3		
		303.2	-4861.3 ± 25.5		3773.0 ± 24.6	-20.6 ± 0.1	51.9 ± 0.2		
Propionate		6	289.0	-2836.5 ± 27.4	-290.2 ± 6.3	6334.0 ± 34.6	-21.0 ± 0.1	62.9 ± 0.3	6230.9 ± 56.3
			293.4	-3383.7 ± 26.6		6212.0 ± 28.9	-21.3 ± 0.1	61.1 ± 0.3	
			298.2	-4848.8 ± 24.5		6180.0 ± 73.1	-21.6 ± 0.1	56.2 ± 0.3	
			303.3	-6851.0 ± 23.6		5881.0 ± 60.7	-21.8 ± 0.1	49.3 ± 0.3	
	7	288.6	-941.8 ± 18.8	-438.1 ± 10.2	6315.0 ± 63.5	-20.9 ± 0.1	69.2 ± 0.3	5650.6 ± 47.8	
		293.2	-3625.8 ± 18.0		5629.3 ± 67.1	-21.0 ± 0.1	59.4 ± 0.3		
		298.1	-3745.7 ± 14.8		5408.0 ± 38.9	-21.3 ± 0.1	58.9 ± 0.2		
		303.2	-7303.3 ± 31.2		4623.0 ± 29.8	-21.2 ± 0.1	45.9 ± 0.3		
	8	288.8	6961.8 ± 21.7	-141.0 ± 7.3	582.3 ± 18.3	-15.3 ± 0.1	77.1 ± 0.2	465.7 ± 9.9	
		293.2	6625.7 ± 27.6		569.0 ± 10.0	-15.4 ± 0.1	75.1 ± 0.3		
		298.1	6521.6 ± 22.8		491.9 ± 13.2	-15.4 ± 0.1	73.6 ± 0.2		
		303.2	4763.5 ± 31.8		484.4 ± 27.8	-15.5 ± 0.1	66.8 ± 0.2		
Butyrate	6	289.1	-1164.8 ± 42.7	-151.9 ± 7.8	524.0 ± 23.5	-15.1 ± 0.1	48.2 ± 0.2	438.6 ± 5.38	
		293.1	-2120.4 ± 30.2		475.8 ± 15.3	-15.0 ± 0.1	43.9 ± 0.1		
		298.2	-2805.0 ± 83.9		386.9 ± 12.8	-14.8 ± 0.1	40.2 ± 0.2		
		303.2	-3253.6 ± 31.7		347.4 ± 11.4	-14.8 ± 0.1	38.1 ± 0.3		
	7	289.7	-899.9 ± 22.3	-161.1 ± 8.2	502.0 ± 10.9	-14.9 ± 0.1	48.3 ± 0.3	495.4 ± 8.41	
		293.9	-2179.4 ± 23.8		476.0 ± 9.3	-15.0 ± 0.1	43.6 ± 0.3		
		298.4	-2370.9 ± 33.4		397.0 ± 11.7	-14.9 ± 0.1	42.0 ± 0.2		
		303.3	-3297.5 ± 50.1		381.1 ± 15.9	-15.0 ± 0.1	38.6 ± 0.2		

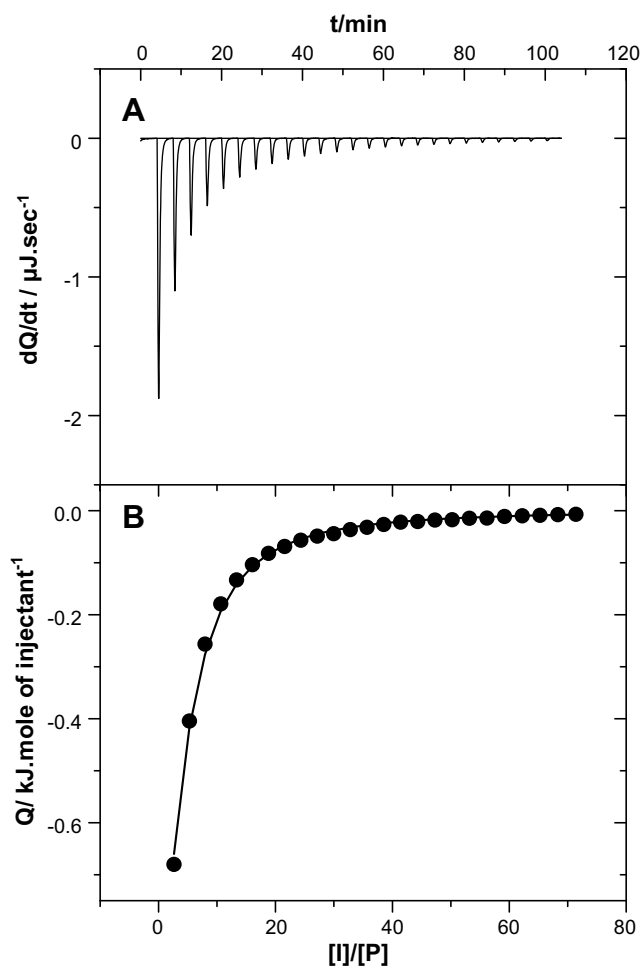


FIGURE 3. Calorimetric titration of the binding of propionate to Atβcar in 100 mM sodium phosphate, 0.5 mM NiCl₂ at pH 7 and $T = 293.15$ K. The experiment consisted of 25 injections of 0.010 cm³ each of a 10.21 mM stock solution of propionate. Propionate was injected into a sample cell (volume = 1.38 cm³) containing 28.22 μM of Atβcar. Injections were at 4-min intervals. The upper panel is the thermogram that shows a typical profile of the binding of propionate to the enzyme. In the lower panel, the plot of total heat evolved per mole of ligand against the molar ratio of inhibitor to enzyme concentration represents the integrated peak areas corrected for heats of dilution. The solid line through the data points represents the line of best fit obtained using ORIGIN 5 software.

enthalpy change obtained. An increase in the length of the apolar side chain of the inhibitor produces a more hydrophobic environment, which would explain the fact that the enthalpy change is more negative for propionate than for acetate and formiate.

For butyrate, the binding constant decreases together with a less exothermic enthalpy. This may be explained by the fact that the binding site of the enzyme could bind with high affinity ligands with three carbon atoms, but when this number is increased the steric impediment decreases the binding constant. This effect is more evident with ligands of five or more carbon atoms, for which binding constants were too small to be detected, (although these compounds are still able to inhibit the enzyme, showing that they bind to the binding site, see table 1). Even though the K values for formiate and butyrate are $\sim 10^2$ M⁻¹, according to the criteria of Turnbull and Daranas [18] these constants could be determined.

Experiments for propionate were carried out at pH 8 to evaluate the effect of pH on the binding process. The results are shown in table 2. At this pH, a high decrease in the binding constant is observed together with a positive enthalpy change. This fact could be explained in terms of the change in the ionisation state of some

amino acids responsible for ligand binding. At this pH, the only amino acid able to change its protonation state (relative to pH 7) is His229, which would not be protonated. Thus, the hydrogen bond could not be formed, changing the forces involved in the binding (a different sign in the enthalpy) and decreasing the affinity of the ligand to the binding site (lower binding constant).

A linear dependence of the binding enthalpy on temperature was observed for the four ligands studied over the temperature range used in ITC experiments. From the slope of the graphical plot of ΔH_b versus temperature, the values of ΔC_p were determined for every ligand studied. These values are shown in table 2. We can appreciate that ΔC_p is negative for all substrate analogues used. Ladbury *et al.* [19] suggest that a negative ΔC_p may be a consequence of high specificity binding, whether at high or low affinity. Negative ΔC_p values indicate changes in hydrophobic and hydrophilic areas buried upon ligand binding, with liberation of water molecules from both the protein and the ligand. Heat capacity changes involved in protein-binding arise from changes in the degree of surface hydration in the free and complex molecules, and to a lesser extent, from changes in molecular vibrations [20,21]. In the association process of a ligand to a protein, a substantial fraction of polar and non-polar surface is buried, and some semi-empirical methods have been developed to calculate the molecular surface buried in the complex. Freire *et al.* [20,22] have suggested the following equation for ΔC_p

$$\Delta C_p = 1.88\Delta ASA_{np} - 1.09\Delta ASA_p \quad (9)$$

and ΔH_{313}

$$\Delta H_{313} = -35.3\Delta ASA_{np} + 131\Delta ASA_p, \quad (10)$$

where ΔC_p , ΔH_{313} , and ΔASA are in J · K⁻¹ · mol⁻¹, J · mol⁻¹, and 10⁻²⁰ m² units, respectively. ΔASA_{np} and ΔASA_p represent the changes in non-polar and polar areas exposed to the solvent (accessible surface area) that take place upon protein ligand binding. The ΔH_{313} is the binding enthalpy at $T = 313$ K, calculated assuming a constant ΔC_p and the experimental heat capacity change. The temperature of 313 K in the expression is the mean value of the denaturation temperatures of the model proteins used in the analysis. Table 3 shows the values obtained for the four ligands. The X-ray crystallographic data of several proteins have been used to calculate the changes in the water-accessible surface areas of both non-polar and polar residues on protein folding. These calculations reveal that the $\Delta ASA_{np}/\Delta ASA_p$ ratio varies between 1.2 and 1.7 [20]. This range is comparable with the mean value for the ratio of $\Delta ASA_{np}/\Delta ASA_p$ of ~ 1.5 (see table 3), calculated for the interactions described in this study.

The values of ΔG were calculated from the microscopic binding constant at each temperature ($\Delta G = -RT \ln K$; see table 2) and are practically independent of temperature, indicating the occurrence of enthalpy–entropy compensation at this pH. This effect seems an almost inevitable property of perturbation of any system com-

TABLE 3

ΔASA values for formiate, acetate, propionate, and butyrate calculated from calorimetric results data at pH 6 and 7

Substrate	pH	ΔASA_{np} (%)	ΔASA_p (%)	$\Delta ASA_{np}/\Delta ASA_p$
Formiate	6	58.8	41.2	1.42
	7	59.3	40.7	1.46
Acetate	6	59.0	41.0	1.44
	7	59.3	40.7	1.45
Propionate	6	58.6	41.4	1.41
	7	60.4	39.6	1.52
Butyrate	6	58.2	41.8	1.39
	7	58.9	41.0	1.44

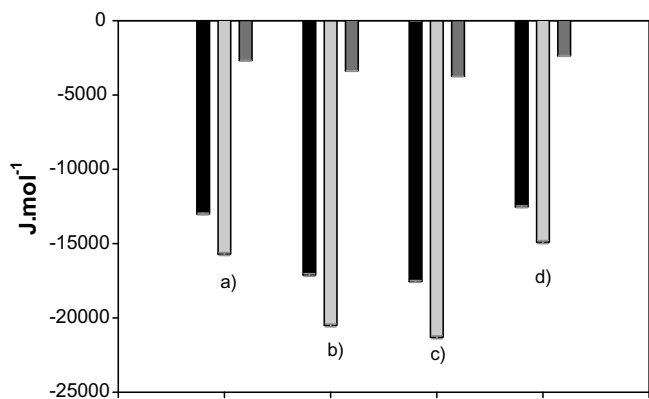


FIGURE 4. Thermodynamic binding parameters ΔH , ΔG , $T\Delta S$ of (a) formiate, (b) acetate, (c) propionate, and (d) butyrate, determined by isothermal titration calorimetry. Black bars, $-T\Delta S$; dark gray bars, ΔH ; and gray bars, ΔG .

prising multiple, weak intermolecular forces [23]. The ΔG is negative in all cases indicating that the binding process for the four ligands is thermodynamically favourable. The most favourable binding process is in the order At β car with propionate > acetate > formiate > butyrate. The entropy change was calculated from the binding enthalpy ($\Delta G = \Delta H_b - T\Delta S$) (table 2). ΔS values are positive at all temperatures studied.

From the dissection of the binding affinity for these inhibitors (figure 4), it can be inferred that the dominant contribution to the Gibbs free energy is the entropy change. When the dominant driving force for binding is a large positive entropy change, this

originates primarily from a large positive solvation entropy due to the burial of a large hydrophobic surface upon binding and a small loss of conformational entropy due to the little flexibility ligands preshaped to the geometry of the binding site [24]. As the main interaction of inhibitors with the enzyme is hydrogen bonding, the positive entropy value together with the negative ΔC_p , generally associated to the burial of hydrophobic surface and liberation of water molecules could be partly explained by a conformational change that would take place when the ligand binds to the enzyme. Similar results were presented for other binds to the enzyme. Similar results were presented for other binds to the enzyme [25,26]. By analogy with the closed structure observed for Sk β as [9], this result points towards a conformational change in At β car comprising closure of the catalytic domain towards the lid domain after substrate binding to Arg291, Asn278, and His229 (figure 1).

We studied whether the presence of the cation in the catalytic centre had any influence on the binding properties of the enzyme (due to conformational changes or structure stabilization). Similar experiments were carried out with the apoenzyme, using formiate, acetate, propionate, and butyrate. The values of the microscopic binding constants at pH 7 and $T = 298$ K were $\{(550.8 \pm 18.6), (4120.5 \pm 38.9), (5260.3 \pm 65.3), \text{ and } (402.8 \pm 20.7)\} \text{ M}^{-1}$, respectively. These values are similar to those obtained for the holoenzyme, indicating that the presence of the cations in the catalytic site of At β car did not significantly affect the binding of the analogues. This fact means that presence of the cation is not indispensable for ligand binding although it is for substrate hydrolysis [17]. The binding of formiate, acetate, propionate, and butyrate to At β car was also measured by intrinsic fluorescence. A decrease in fluorescence as a function of ligand concentration was obtained at $T = 298$ K in the buffer 100 mM sodium phosphate, 0.5 mM NiCl₂

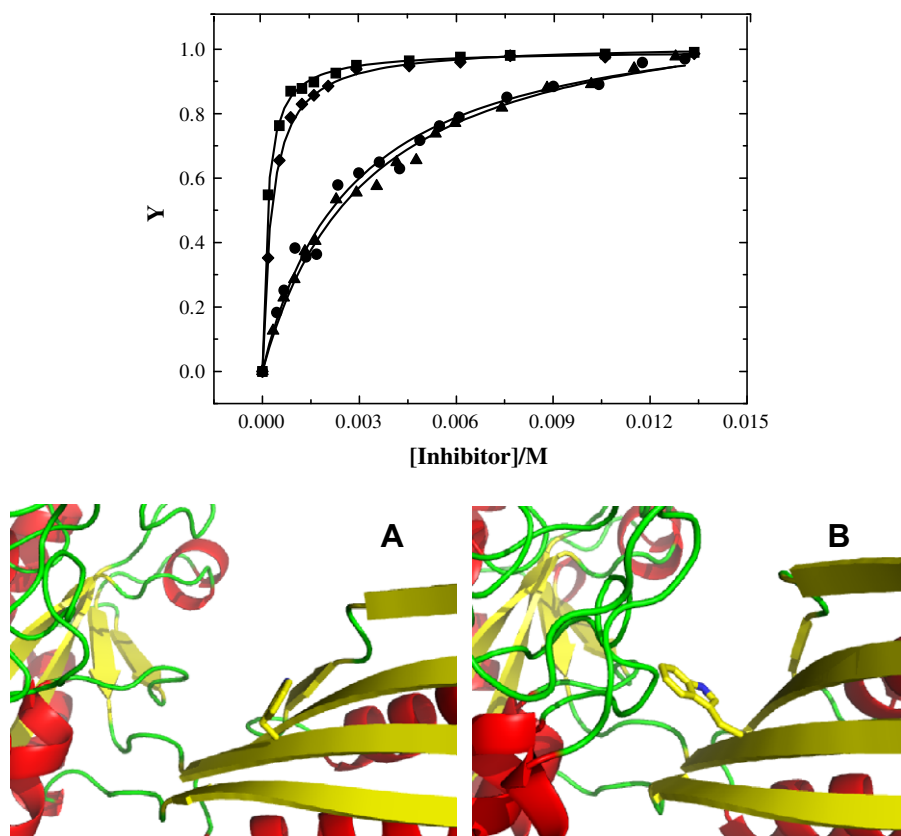


FIGURE 5. Top – Plot of saturation fraction Y against concentration of the inhibitor to show the binding titration of formiate, acetate, propionate, and butyrate to At β car. The fluorescence titration was performed in 100 mM sodium phosphate, 0.5 mM NiCl₂, pH 7 and $T = 298.15$ K. Enzyme concentrations were 0.3 μM . Titrations were carried out by addition of either (0.005 or 0.010) cm^3 of stock solutions at concentrations of 100 mM of formiate (\bullet), 103.5 mM of butyrate (\blacktriangle), 93.5 mM of acetate (\blacklozenge), or 74.8 mM of propionate (\blacklozenge). Bottom – Models of (A) open and (B) closed monomer of At β car on the basis of Sk β as X-ray structures, showing how Trp218 might be responsible for the differences in fluorescence emission.

TABLE 4Thermodynamic parameters and binding constants determined by ITC for the binding of different substituted inhibitors to At β car at $T = 298$ K and pH 7

Substrate	$\Delta H/(\text{J} \cdot \text{mol}^{-1})$	K/M^{-1}	$\Delta G/(\text{kJ} \cdot \text{mol}^{-1})$	$\Delta S/(\text{J} \cdot \text{K}^{-1} \cdot \text{mol}^{-1})$
Isobutyric acid	-3259.2 ± 35.3	1899.0 ± 28.9	-18.7 ± 0.1	51.8 ± 0.2
2-Phenylpropionic acid	-2303.2 ± 54.7	1140.0 ± 49.5	-17.4 ± 0.1	50.7 ± 0.2
3-Phenylpropionic acid	-609.5 ± 11.9	100.6 ± 2.3	-11.2 ± 0.1	35.5 ± 0.3
2-Methylbutyric acid	-1930.6 ± 35.6	250.3 ± 12.8	-13.7 ± 0.1	39.5 ± 0.2
2-Phenylbutyric acid	-998.3 ± 42.5	115.4 ± 15.5	-11.7 ± 0.3	35.9 ± 0.9
3-Methylbutyric acid	N.D.	N.D.		
3-Phenylbutyric acid	N.D.	N.D.		
Valeric acid	N.D.	N.D.		

N.D.: no binding is detected by ITC.

at pH 7 (similar results were obtained by excitation at (280 and 295) nm). Figure 5 represents the saturation fraction versus concentration of formiate, acetate, propionate, and butyrate, and the results fit to a model of two equal and non-interacting sites (figure 5). The good fit of the experimental curve is an indication of the absence of cooperativity in the binding of these ligands to At β car, and yields binding constant values (K) in agreement with data obtained by ITC (table 2). These results corroborate the non-cooperativity effect hypothesized for Sk β as by Lundgren *et al.* [9]. A tryptophan (Trp218) appears in the region where the binding site is allocated, and thus it must be buried by the conformational change triggered upon inhibitor binding (figure 5 bottom). The decrease in fluorescence intensity due to inhibitor binding could be explained by the proximity of this residue to the negative charge of the carboxylate moiety of Asp289 in the closed structure (or even to that of the inhibitor), thereby reducing its fluorescence quantum yield [27,28].

3.5. Binding of 2- and 3-substituted carboxylic acids

ITC experiments were carried out at pH 7 and $T = 298$ K with several ramified carboxylic acids to evaluate the influence of the ramification in the binding process (table 4). The presence of a methyl or a phenyl group in position 2 of propionate or butyrate lowered the affinity constant, with a larger decrease for the latter (table 4). In all cases, binding is enthalpically and entropically favoured. The decrease in affinity constant due to the presence of

TABLE 5Thermodynamic parameters of the urea-induced denaturation of At β car at $T = 298$ K

pH	$m/(\text{kJ} \cdot \text{mol}^{-1} \cdot \text{M}^{-1})$	$C_{1/2}/\text{M}$	$\Delta G_w/(\text{kJ} \cdot \text{mol}^{-1})$
6	3.1 ± 0.1	2.6 ± 0.1	32.7 ± 0.9
7	3.4 ± 0.1	4.1 ± 0.2	38.4 ± 1.1
8	2.4 ± 0.1	1.6 ± 0.1	28.4 ± 0.5

ramification could be explained by steric impediment due to the presence of a group in position 2. This effect would be higher when the ramification group is bulkier, as can be seen from the decrease in binding affinity constant when there is a phenyl rather than a methyl group in position 2. This decrease in affinity is caused by a less favourable enthalpic contribution (table 4).

Substitution in position 3 by a phenyl group of propionate results in a 10-fold decrease of the binding constant compared to the same substitution in position 2. Substitution in position 3 by a methyl or a phenyl group of butyrate resulted in negligible binding under the experimental conditions (table 4).

3.6. Stability of At β car at several pHs

In order to study the influence of pH on the stability of the enzyme we carried out chemical-denaturation experiments in the presence of Ni^{2+} using urea as denaturant. The emission fluorescence spectrum of At β car showed a maximum at 350 nm, arising from different contributions of the seven tyrosines located at positions 82, 154, 156, 166, 189, 192, and 350 and eight tryptophans located at positions 15, 51, 128, 175, 217, 218, 365, and 395. The urea-denaturation of At β car was monitored by observing the changes in fluorescence at the maximum of the spectrum (similar results were obtained by excitation at (280 and 295) nm). Profiles of fluorescence intensity versus denaturant concentration were obtained for the enzyme at pH (6, 7, and 8) (figure 6).

The results were fitted to a two-state model in which the fluorescence of the folded and unfolded states is dependent on denaturant concentration [16,29]. Gel filtration experiments at different urea concentrations showed that only two significantly populated species were in equilibrium during the denaturation process, the dimer, and the unfolded monomer (figure 6, inset). The results obtained are shown in table 5. The conformational transition induced by increasing the urea concentration and monitored by the decrease in fluorescence intensity had a sigmoid shape (figure 6). The values of m , $C_{1/2}$, and ΔG_w are shown in table 5. The enzyme is more stable at pH 7 than at pH 6 or 8 (with a difference of (5.7 and 10) $\text{kJ} \cdot \text{mol}^{-1}$, respectively).

4. Conclusions

ITC and fluorescence studies were made of the binding to At β car of different carboxylic acids that differ in chain length and the position and kind of ramification. The results are adjusted to a model

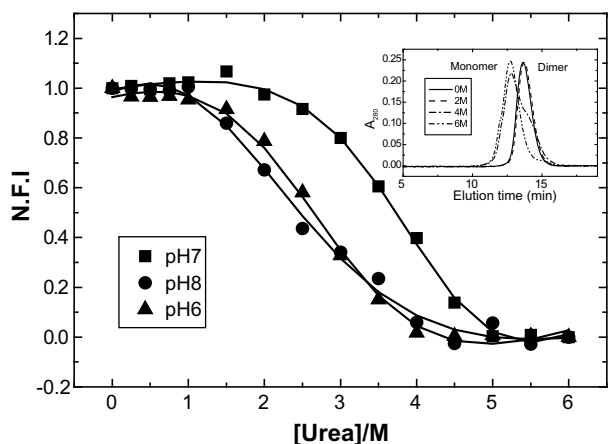


FIGURE 6. Plot of the intrinsic fluorescence intensity At β car as a function of Urea concentration. The intrinsic fluorescence intensity spectra of the enzyme were obtained after equilibrium had been achieved at the indicated denaturant concentrations in 100 mM sodium phosphate, 0.5 mM NiCl_2 for pH 6 ▲, pH 7 ■, and pH 8 ●, and $T = 298.15$ K. Within the inset, the plot of absorbance against elution time shows the gel filtration profiles of At β car at pH 7 and $T = 298.15$ K at four different concentrations of urea: 0 M —, 2 M ---, 4 M ---, and 6 M ---.

of two equal and independent sites. With the results obtained in this paper, we can conclude that the binding of the different inhibitors to the enzyme produces a conformational change in the protein in agreement with the available structural data for the homologous Skβas enzyme. Negative enthalpy values show that hydrogen bonding and salt bridge are responsible for ligand binding to the enzyme, and the amino acids involved are Arg291 of one monomer and His229 and Asn278 of the other monomer. Ramification in position 2 or 3 in the carboxylic acids decreases the affinity to the enzyme, and this is more evident when the ramification group is bulky. These two facts can be explained in terms of steric impediment in the active site of the enzyme. Stability studies in presence of a denaturant indicate that its stability is higher at pH 7 than pH 6 or 8.

Acknowledgements

This work was supported by the Spanish Ministry of Education and Science BIO2007-67009, by the Spanish Ministry of Education and Science and the European Social Fund through research Grant BES-2008-003751 and Andalusian Regional Council of Innovation, Science and Technology P07-CVI-2651 projects. The authors thank Andy Taylor for critical discussion of the manuscript and Pedro Madrid-Romero for technical assistance.

References

- [1] J.E. Cronan, K.J. Little, S. Jackowski, *J. Bacteriol.* 149 (1982) 916–922.
- [2] S. Lundgren, Z. Gojkovic, J. Piskur, D. Dobritzsch, *J. Biol. Chem.* 278 (2003) 51851–51862.
- [3] T.A. Walsh, S.B. Green, I.M. Larrinua, P.R. Schmitzer, *Plant Physiol.* 125 (2001) 1001–1011.
- [4] J. Ogawa, S. Shimizu, *Eur. J. Biochem.* 223 (1994) 625–630.
- [5] A.H. Van Gennip, H. Van Lenthe, N.G.G.M. Abeling, E.G. Scholten, A.B.P. Van Kuilenburg, *J. Inher. Metab. Dis.* 20 (1997) 379–382.
- [6] J.D. Thompson, D.G. Higgins, T.J. Gibson, *Nucleic Acids Res.* 22 (1994) 4673–4680.
- [7] P. Gouet, E. Courcelle, D.I. Stuart, F. Metz, *Bioinformatics* 15 (1999) 305–308.
- [8] T. Schwede, J. Kopp, N. Guex, M.C. Peitsch, *Nucleic Acids Res.* 31 (2003) 3381–3385.
- [9] S. Lundgren, B. Andersen, J. Piskur, D. Dobritzsch, *J. Biol. Chem.* 282 (2007) 36037–36047.
- [10] R.A. Laskowski, V.V. Chistyakov, J.M. Thornton, *Nucleic Acids Res.* 33 (2005) D266–D268.
- [11] R.A. Laskowski, M.W. MacArthur, D.S. Moss, J.M. Thornton, *J. Appl. Crystallogr.* 26 (1993) 283–291.
- [12] N. Guex, M.C. Peitsch, *Electrophoresis* 18 (1997) 2714–2723.
- [13] W. L. Delano, The PyMOL Molecular Graphics System, 2002, on World Wide Web <<http://www.pymol.org>>.
- [14] M. Andújar-Sánchez, A. Cámara-Artigas, V. Jara-Pérez, *Biophys. Chem.* 111 (2004) 183–189.
- [15] T. Wiseman, S. Williston, J.F. Brandts, L.N. Lin, *Anal. Biochem.* 179 (1989) 131–137.
- [16] S. Sinha, N. Mitra, G. Kumar, K. Bajajand, A. Surolia, *Biophys. J.* 88 (2005) 1300–1310.
- [17] S. Martínez-Rodríguez, M. Andujar-Sánchez, J.M. Clemente-Jiménez, V. Jara-Pérez, F. Rodríguez-Vico, F.J. Las Heras-Vázquez, *Biochimie* 88 (2006) 837–847.
- [18] W.C. Turnbull, A.H. Daranas, *J. Am. Chem. Soc.* 125 (2003) 14859–14866.
- [19] E. Ladbury, J.G. Wright, J.M. Sturtevant, P.B. Sigler, *J. Mol. Biol.* 238 (1994) 669–681.
- [20] K.P. Murphy, E. Freire, *Adv. Prot. Chem.* 43 (1992) 313–361.
- [21] J.R. Livingstone, R.S. Spolar, M.T. Record Jr., *Biochemistry* 31 (1992) 3947–3955.
- [22] V.J. Hilser, J. Gomez, E. Freire, *Proteins* 26 (1996) 123–133.
- [23] J.D. Dunitz, *Chem. Biol.* 2 (1995) 709–712.
- [24] A. Velazquez-Campoy, I. Luque, M.J. Todd, M. Milutinovich, Y. Kiso, E. Freire, *Protein Sci.* 9 (2000) 1801–1809.
- [25] K. Bhadra, M. Maiti, G.S. Kumar, *Biochim. Biophys. Acta* 1780 (2008) 298–306.
- [26] M.J. Todd, I. Luque, A. Velazquez-Campoy, E. Freire, *Biochemistry* 39 (2000) 11876–11883.
- [27] J.J. Lacapère, G. Boulla, F.E. Lund, J. Primack, N. Oppenheimer, F. Schuber, P. Deterre, *Biochim. Biophys. Acta* 1652 (2003) 17–26.
- [28] H.S. Park, J.W. Park, *Biochim. Biophys. Acta* 1387 (1998) 406–414.
- [29] C.N. Pace, *Methods Enzymol.* 131 (1986) 266–280.